properties of the ES complexes are mimicked by synthetic complexes with either monodentate and chelated catecholate. Catecholate-to-iron(III) charge-transfer transitions are observed near 600 nm and catecholate binding results in blue shifts of the salen-to-iron(III) charge-transfer band. However, neither model complex adequately reproduces the spectral properties observed for the enzyme complexes. Though the Raman spectra of the ES complexes are modeled well by [Fe(salen)cat]$^-$, the excitation profiles of the ES complexes are better matched by that of Fe(salen)catH. Thus resonance Raman data to date cannot distinguish the mode of catechol binding to the enzymes. The catecholate coordination mode in the ES complexes has been elucidated by using paramagnetic NMR spectroscopy based on the same models. The catecholate was found to be monodentate in the CTD ES complex and chelated in the PCD ES complex.[63]

Our model studies support the proposed dioxygenase reaction mechanism, which does not involve the ferrous oxidation state.[23] Mössbauer spectroscopy has conclusively shown that no ferrous species can be discerned in the native enzymes, the enzyme-substrate complexes, and the steady-state intermediates generated from PCD, 3,4-dihydroxyphenylpropionate, and O_2[24] and from CTD, pyrogallol, and O_2.[64] The presence of tyrosine ligands makes the possibility of the fleeting participation of iron(II) in the reaction cycle quite unlikely. Phenolate ligands favor the ferric oxidation state and lower the Fe^{III}/Fe^{II} reduction potential. The coordination of catecholate, whether as a monodentate or chelated ligand, introduces yet another phenolate moiety into the iron coordination sphere and further lowers the potential. The blue shift of the tyrosinate-to-iron(III) charge-transfer band observed upon substrate binding to the enzymes is indicative of the lowered potential. In addition, intermediates observed in rapid kinetic studies of the catechol dioxygenases all exhibit visible spectra which indicate the persistence of the tyrosinate-to-iron(III) charge-transfer transition throughout the cycle.[64-66] The substantial blue shifts exhibited by some of these complexes suggest structures for the organic intermediates involved in the reaction. When the ES complex is exposed to oxygen, the catecholate charge-transfer band disappears, while the blue-shifted tyrosinate band is retained.[64-66] Since the tyrosinate-to-iron(III) charge-transfer bands of the catechol dioxygenase complexes appear to shift according to the spectrochemical series derived for the model series,[29] the blue shift observed for the first intermediate indicates that the catecholate has been converted to a fairly basic ligand, which would be consistent with alkoxide or peroxide species in the proposed mechanism.[23] Similar blue shifts have been reported for the binding of 2-hydroxypyridine *N*-oxides to PCD and CTD; these substrate analogues are proposed to mimic the ketonized form of the substrate and the blue shift is suggested to result from the binding of the *N*-oxide to the iron.[67,68]

In conclusion, our model studies have provided useful insights into the coordination chemistry of iron-phenolate complexes. We have applied these to the understanding of the active site and mechanism of the catechol dioxygenases. They should also be helpful in interpreting the spectral properties of other iron-tyrosinate proteins.

Acknowledgment. This work was supported by grants from the National Institutes of Health and the National Science Foundation. L.Q. is a Fellow of the Alfred P. Sloan Foundation (1982-1986) and the recipient of an NIH Research Career Development Award (1982-1987). We thank R. H. Heistand, R. B. Lauffer, and especially Professor Harry B. Gray for valuable discussions.

(62) Que, L., Jr., unpublished observations.
(63) Lauffer, R. B.; Que, L., Jr. *J. Am. Chem. Soc.* **1982**, *104*, 7324-7325.
(64) Que, L., Jr.; Mayer, R. *J. Am. Chem. Soc.* **1982**, *104*, 875-877.
(65) Bull, C.; Ballou, D. P.; Otsuka, S. *J. Biol. Chem.* **1981**, *256*, 12681-12686.
(66) Walsh, T. A.; Ballou, D. P.; Mayer, R.; Que, L, Jr. *J. Biol. Chem.* **1983**, *258*, 14422-14427.
(67) May, S. W.; Oldham, C. D.; Mueller, P. W.; Padgette, S. R.; Sowell, A. L. *J. Biol. Chem.* **1982**, *257*, 12746-12751.
(68) Whittaker, J. W.; Lipscomb, J. D. *J. Biol. Chem.* **1984**, *259*, 4476-4486.

Kinetics and Thermodynamics of Intra- and Intermolecular Carbon-Hydrogen Bond Activation

William D. Jones* and Frank J. Feher

Contribution from the Department of Chemistry, University of Rochester, Rochester, New York 14627. *Received May 21, 1984*

Abstract: The preference for intra- and intermolecular C-H bond activation has been determined by equilibration of the complex $(C_5Me_5)Rh(PMe_2CH_2C_6H_5)(C_6H_5)H$ and its cyclometalated analogue $(C_5Me_5)\overline{Rh(PMe_2CH_2C_6H_4)}H$ in neat benzene at 51.2 °C (K_{eq} = 36.7, $\Delta G°$ = -2.32 kcal/mol). By monitoring the approach to equilibrium over a 40 °C temperature range, the difference between the activation parameters for intra- and intermolecular activation by the 16-electron intermediate $[(C_5Me_5)Rh(PMe_2CH_2C_6H_5)]$ can be obtained (intra-inter): $\Delta\Delta H^‡$ = 1.7 ± 0.8 kcal/mol; $\Delta\Delta S^‡$ = 4.5 ± 2.5 eu. At 25 °C, this corresponds to a 1.86:1 kinetic preference for intermolecular activation of the neat benzene solvent by the coordinatively unsaturated intermediate $[(C_5Me_5)Rh(PMe_2CH_2C_6H_5)]$ over intramolecular cycloaddition. The effect of solvent concentration on activation selectivity is discussed. A comparison with intra- and intermolecular alkane activation is made by equilibrating the complex $(C_5Me_5)\overline{Rh(PMe_2CH_2CH_2CH_2)}H$ with benzene and by examining the kinetics of cyclometalation vs. alkane activation. These studies reveal the same general trend with regard to thermodynamic and kinetic selectivity in alkanes and arenes: while there is little kinetic selectivity between intra- and intermolecular reactions involving neat solvent, there is a moderate thermodynamic preference for the intramolecular activation.

The activation of carbon-hydrogen bonds by homogeneous transition-metal complexes is a topic that has received a great deal of attention recently. Much of this interest arises from the recent reports that indicate that even the C-H bonds of alkanes can

0002-7863/85/1507-0620$01.50/0

undergo oxidative addition to a metal center.[1] Until the appearance of these reports there existed only examples of intramolecular alkane activation,[2] although numerous examples of both intra- and intermolecular arene activation were known.[3] The absence of intermolecular alkane activation suggested that perhaps this particular process was kinetically and/or thermodynamically unfavorable for all transition-metal complexes.

We have recently reported a full kinetic and thermodynamic study of the intermolecular activation of arene C–H bonds by $[(C_5Me_5)Rh(PMe_3)]$ that indicated that arenes were activated by way of an η^2-arene intermediate formed in the rate-determining step to oxidative addition.[4] This barrier to coordination was comparable to the barrier to intermolecular alkane activation in this system, thereby allowing competitive activation of both arene and alkane bonds. This result also indicates that there is only a slight preference for arene activation over alkanes and that the paucity of complexes that activate alkanes is not due to any inherent difference in the kinetics of arene and alkane activation. This conclusion stands in direct opposition to the numerous examples of compounds that activate exclusively intramolecular alkane C–H bonds.[2]

Several recent examples of intramolecular activation are shown in Scheme I. Metalation of sp^3-hybridized C–H bonds of alkyl groups attached to cyclopentadienyl rings, phosphines, and the

Scheme I. Examples of Intramolecular Activation

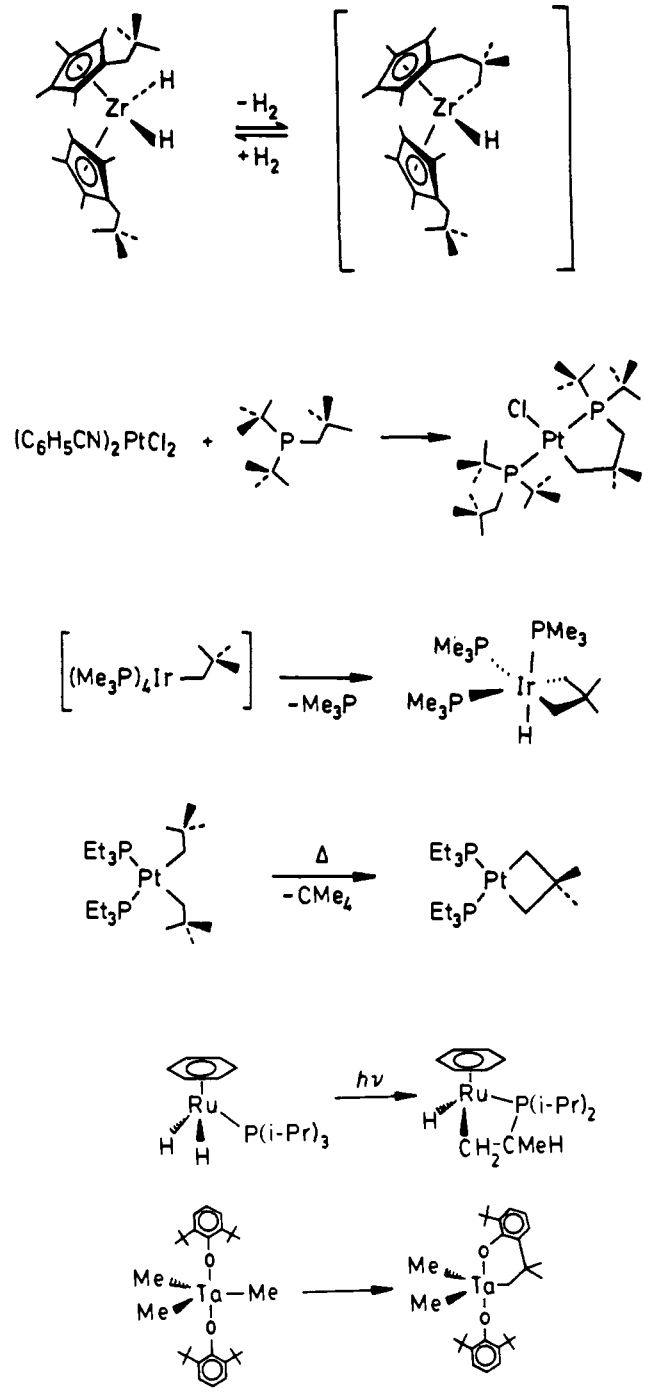

metal itself have been observed. The incidence of examples of intramolecular activation led to the speculation that perhaps entropy played a major role in the difference between intra- and intermolecular oxidative addition reactions.[2f] Estimates of the contribution of the entropy of activation to the free energy of activation ($-T\Delta S^{\ddagger}$) range up to 10 kcal/mol, based upon the general eq 1 and 2 below. If it is assumed that the difference between the enthalpies of activation ($\Delta\Delta H^{\ddagger}$) is near zero for these reactions (i.e., the bond energies are the same in reactions 1 and 2 and there is negligible ring strain or nonbonded H–H interactions in the cyclometallated species) and that there is a difference of 10–30 eu between the entropies of activation of the intermolecular and intramolecular reactions,[5a] then a $\Delta\Delta G^{\ddagger}$ of 3–9 kcal/mol can

(1) (a) Crabtree, R. H.; Mihelcic, J. M.; Quirk, J. M. *J. Am. Chem. Soc.* **1979**, *101*, 7738–7740. Crabtree, R. H.; Mellea, M. F.; Mihelcic, J. M.; Quirk, J. M. *J. Am. Chem. Soc.* **1982**, *104*, 107–113. Crabtree, R. H.; Demou, P. C.; Eden, D.; Mihelcic, J. M.; Parnell, C. A.; Quirk, J. M.; Morris, G. E. *J. Am. Chem. Soc.* **1982**, *104*, 6994–7001. (b) Baudry, D.; Ephritikhine, M.; Felkin, H. *J. Chem. Soc., Chem. Commun.* **1980**, 1243–1244. Baudry, D.; Ephritikhine, M.; Felkin, H.; Zakrzewski, J. *J. Chem. Soc., Chem. Commun.* **1982**, 1235–1236. (c) Shilov, A. G.; Shteinman, A. A. *Coord. Chem. Rev.* **1977**, *24*, 97–143. (d) Janowicz, A. H.; Bergman, R. G. *J. Am. Chem. Soc.* **1982**, *104*, 352–354. Janowicz, A. H.; Bergman, R. G. *J. Am. Chem. Soc.* **1983**, *105*, 3929–3939. Wax, M. J.; Stryker, J. M.; Buchanan, J. M.; Kovac, C. A.; Bergman, R. G. *J. Am. Chem. Soc.* **1984**, *106*, 1121–1122. (e) Hoyano, J. K.; Graham, W. A. G. *J. Am. Chem. Soc.* **1982**, *104*, 3723–3725. Hoyano, J. K.; McMaster, A. D.; Graham, W. A. G. *J. Am. Chem. Soc.* **1983**, *105*, 7190–7191. (f) Watson, P. L. *J. Am. Chem. Soc.* **1983**, *105*, 6491–6493. (g) Bercaw, J. E. "11th International Conference on Organometallic Chemistry", Atlanta, GA, Oct. 10–14, 1983. (h) Fendrick, C. M.; Marks, T. J. *J. Am. Chem. Soc.* **1984**, *106*, 2214–2216. (i) Kitajima, N.; Schwartz, J. *J. Am. Chem. Soc.* **1984**, *106*, 2220–2222.

(2) (a) Goel, R. G.; Montemayor, R. G. *Inorg. Chem.* **1977**, *16*, 2183–2186. (b) Cheney, A. J.; Mann B. E.; Shaw, B. L.; Slade, R. M. *J. Chem. Soc., A* **1971**, 3833–3842. Empsall, H. D.; Hyde, E. M.; Shaw, B. L. *J. Chem. Soc., Dalton Trans.* **1975**, 1690–1696. Mason, R.; Textor, N. A.-S.; Shaw, B. L. *J. Chem. Soc., Chem. Commun.* **1976**, 292–293. (c) Kiffen, A. A.; Masters, C.; Raynand, L. *J. Chem. Soc., Dalton Trans.* **1975**, 853–857. (d) Anderson, R. A.; Jones, R. A.; Wilkinson, G. *J. Chem. Soc., Dalton Trans.* **1978**, 446–453. Jones, R. A.; Wilkinson, G. *J. Chem. Soc., Dalton Trans.* **1979**, 472–477. (e) Tulip, T. H.; Thorn, D. L. *J. Am. Chem. Soc.* **1981**, *103*, 2488–2490. (f) Foley, P.; Whitesides, G. M. *J. Am. Chem. Soc.* **1979**, *101*, 2732–2733. DiCosimo, R.; Moore, S. S.; Sowinski, A. F.; Whitesides, G. M. *J. Am. Chem. Soc.* **1982**, *104*, 124–133. (g) McAlister, D. R.; Erwin, D. K.; Bercaw, J. E. *J. Am. Chem. Soc.* **1978**, *100*, 5966–5968. (h) Kletzin, H.; Werner, H. *Angew. Chem., Int. Ed. Engl.* **1983**, *22*, 873–874. (i) Hietkamp, S.; Stufkens, D. J.; Vrieze, K. *J. Organomet. Chem.* **1978**, *152*, 347–357. (j) Brookhart, M.; Green, M. L. H. *J. Organomet. Chem.* **1983**, *250*, 395–408. (k) Chamberlain, L.; Keddington, J.; Rothwell, I. P.; Huffman, J. C. *Organometallics* **1982**, *1*, 1538–1540.

(3) (a) Parshall, G. W. *Acc. Chem. Res.* **1970**, *3*, 139–141. Werner, R.; Werner, H. *Angew. Chem., Int. Ed. Engl.* **1981**, *20*, 793–794. Parshall, G. W. *Acc. Chem. Res.* **1975**, *8*, 113–117. Green, M. A.; Huffman, J. C.; Caulton, K. G. *J. Am. Chem. Soc.* **1981**, *103*, 695–696. Green, M. L. H. *Pure Appl. Chem.* **1978**, *50*, 27–35. Rausch, M. D.; Gastinger, R. G.; Gardener, S. A.; Brown, R. K.; Wood, J. A. *J. Am. Chem. Soc.* **1977**, *99*, 7870–7876. Grebenik, P. D.; Green, M. L. H.; Izquierdo, A. *J. Chem. Soc., Chem. Commun.* **1981**, 186–187. Gell, K. I.; Schwartz, J. *J. Am. Chem. Soc.* **1981**, *103*, 379–384. Gustavson, W. A.; Epstein, P. S.; Curtis, M. D. *Organometallics* **1982**, *1*, 884–885. Diamond, S. E.; Szalkiewcz, A.; Mares, F. *J. Am. Chem. Soc.* **1979**, *101*, 490–491. Horino, H.; Inoue, N. *Tetrahedron Lett.* **1979**, *26*, 2403–2406. Fujiwara, Y.; Kawauchi, T.; Taniguchi, H. *J. Chem. Soc., Chem. Commun.* **1980**, 220–221. Cooper, N. J.; Green, M. L. H.; Mahtab, R. *J. Chem. Soc., Dalton Trans.* **1979**, 1557–1562. Morris, R. H.; Shiralian, M. *J. Organomet. Chem.* **1984**, *260*, C47–C51. (b) Ryabov, A. D.; Sakodinskaya, I. K.; Yatsimirsky, A. K., Moscow State University, submitted to *J. Chem. Soc., Dalton Trans.*

(4) (a) Jones, W. D.; Feher, F. J. *J. Am. Chem. Soc.* **1982**, *104*, 4240–4242. (b) Jones, W. D.; Feher, F. J. *Organometallics* **1983**, *2*, 686–687. (c) Jones, W. D.; Feher, F. J. *J. Am. Chem. Soc.* **1984**, *106*, 1650–1663. (d) Jones, W. D.; Feher, F. J. *Inorg. Chem.* **1984**, *23*, 2376–2388.

(5) (a) Ibers, J. A.; DiCosimo, R.; Whitesides, G. *Organometallics* **1982**, *1*, 13–20. (b) Reamey, R. H.; Whitesides, G. M. *J. Am. Chem. Soc.* **1984**, *106*, 81–85. (c) Bruice, T. C. *The Enzymes* **1970**, *2*, 217–252. (d) Koshland, D. E. *J. Theor. Biol.* **1962**, *2*, 75–86.

be estimated for these two reactions.[2f]

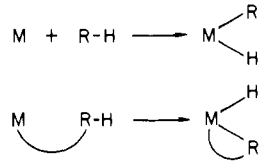

(1)

(2)

When the intermolecular reaction involves activation of the solvent, the high local concentration of solvent molecules should overcome the unfavorable effect of the translational entropy of the intermolecular reaction, as has been calculated by Whitesides[5b] and Bruice.[5c] In practice, however, activation of neat alkane solvent by $[Pt(PEt_3)R_2]$ was not observed by Whitesides under conditions that led to intramolecular activation.[2f] In contrast, Marks[1d] has observed exclusive intermolecular activation of methane by the complex $(C_5Me_5)_2Th(CH_2CMe_2CH_2)$ but competitive intramolecular activation in $(C_5Me_5)_2Th(CH_2CMe_3)_2$. Bergman[1c] reported both intra- and intermolecular activation upon irradiating $(C_5Me_5)Ir(PPh_3)H_2$ in benzene.[1d] Rothwell has observed only intramolecular activation in $Ta[OC_6H_3(t\text{-}Bu)_2]_2Me_3$.[2k] A complete study of the thermodynamics of cyclometalation to form 4-, 5-, and 6-membered rings has also been reported by Whitesides, but no comparison with intermolecular activation could be made.[2f] Ryabov has investigated the relative rates and activation parameters for the cyclometalation of dimethylbenzylamine attached to Pd(II), but the slower intermolecular reaction with benzene required a different solvent.[3b] Werner has seen intramolecular cyclometalation of a phosphine isopropyl group by ruthenium, but only benzene was activated intermolecularly.[2h] It therefore became obvious that an experimental estimation of the difference in the entropies of the intra- and intermolecular reactions would be useful in interpreting the selectivities exhibited by a given system.

Obtaining both the kinetic and thermodynamic preferences for C–H bond activation by a single coordinatively unsaturated metal complex is the subject of this report. The compounds chosen for this study are those that can form unstrained 5-member metallocycles, and the reactions corresponding to aryl C–H bond activation are indicated in eq 3 and 4. The experiments to be

(3)

(4)

presented here indicate that intramolecular activation is thermodynamically favored over intramolecular oxidative addition even when the intermolecular reaction involves neat solvent. Unexpectedly, the *kinetic* selectivity for intramolecular oxidative addition is found to be slightly less favorable than that for activation of the neat solvent. Furthermore, temperature-dependent rate studies reveal that entropic differences do *not* play a major role in determining whether intramolecular C–H bond activation is favored over intermolecular reactions involving pure solvent.

Results and Discussion

A. Preparation and Thermodynamic Stability of $(C_5Me_5)Rh(PMe_2CH_2Ph)(Ph)H$. Employing the experimental methodology described earlier,[4] reaction of a solution of $[(C_5Me_5)RhBr_2]_2$ with 2 equiv of PMe_2CH_2Ph produces $(C_5Me_5)Rh(PMe_2CH_2Ph)Br_2$ in quantitative yield. Upon treatment with 1 equiv of C_6H_5MgBr in THF solution, the complex $(C_5Me_5)Rh(PMe_2CH_2Ph)(C_6H_5)Br$ is isolated in 96% yield. This product is then reacted with $Na^+[H_2Al(OCH_2CH_2OMe)_2]^-$, producing the phenyl hydride

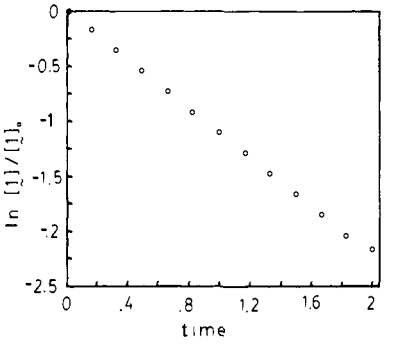

Figure 1. Kinetics of benzene elimination from $(C_5Me_5)Rh(PMe_2CH_2Ph)(C_6H_5)H$ in cyclohexane-d_{12} at 332.0 K.

complex $(C_5Me_5)Rh(PMe_2CH_2Ph)(C_6H_5)H$ (**1**). The product is identified on the basis of its characteristic ^1H NMR spectrum (Table I) and subsequent reaction chemistry.

Thermolysis of **1** in cyclohexane-d_{12} solution at 58.8 °C results in a clean first-order reductive elimination of benzene (Table II, entry 8), producing the ortho-metalated species $(C_5Me_5)Rh(PMe_2CH_2C_6H_4)H$ (**2**) (Figure 1). The reaction goes to completion. A similar thermolysis in benzene solvent at 51.2 °C also results in a first-order elimination of benzene, but it does not quite go to completion. Instead, the equilibrium shown in eq 5 is

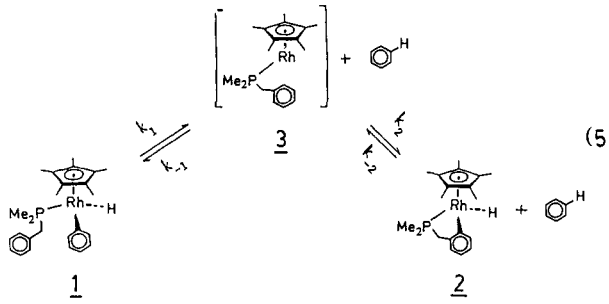

(5)

established with a 97.3:2.65 ratio of **2**:**1**. If the concentrations of **1**, **2**, and C_6H_6 are expressed as mole fractions, then $K_{eq} = 36.7$ (molar $K_{eq} = 397$ M). This corresponds to a $\Delta G°$ of −2.32 (2) kcal/mol for the standard state of neat benzene (−3.86 kcal/mol for 1 M benzene standard state).[6] For other benzene concentrations, the free energy change for eq 5 varies according to eq 6, where $\chi_{benzene}$ is the mole fraction of benzene.

$$\Delta G = \Delta G° \text{ (neat benzene)} + RT \ln (\chi_{benzene}) \qquad (6)$$

The choice of neat benzene as the standard state for the calculations in this paper bears some comment. From eq 6, the standard state for 1 M benzene lies ~1.5 kcal/mol below that for neat benzene solvent. The latter standard state is appropriate to use in these discussions since (1) most experiments were carried out in neat solvent, thereby keeping secondary solvation effects to a minimum, (2) the molarity of benzene changes with temperature ($d = 0.9007 - 0.0010834T$ (°C), or 11.2 M at 25 °C), whereas the mole fraction does not, and (3) the chemically most biased system for demonstrating intermolecular activation involves neat solvent, not the 1 M standard state commonly applicable to solute–solute equilibria. The thermodynamics for the 1 M standard state is useful for comparison with other known chemical systems and therefore will also be presented in the discussion that follows.

Treatment of compound **2** with $CHBr_3$ produces the corresponding bromide complex, $(C_5Me_5)Rh(PMe_2CH_2C_6H_4)Br$ in high yield. An X-ray structural determination of the molecule confirms that the ortho C–H bond of the aromatic ring has been activated (Figure 2). Relevant bond distances and angles are given in Table III. The metallocycle ring is nearly planar, and since the C1–C2–C7 bond angle deviates only 2.6° from ideality, the strain energy of the ring must be quite small.[7] Consequently $\Delta H°$ in eq 4 for intramolecular activation will be expected to be

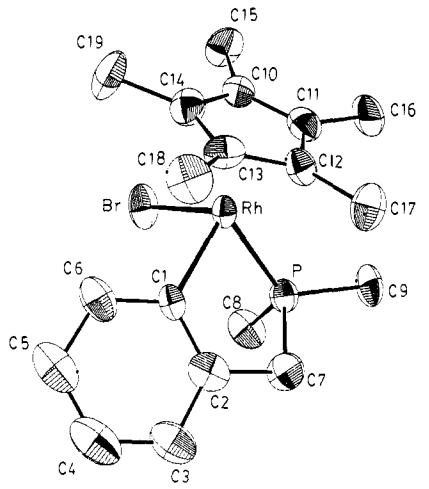

Figure 2. ORTEP drawing of $(C_5Me_5)\overline{Rh(PMe_2CH_2C_6H_4)}Br$. The ellipsoids are shown at the 50% probability level.

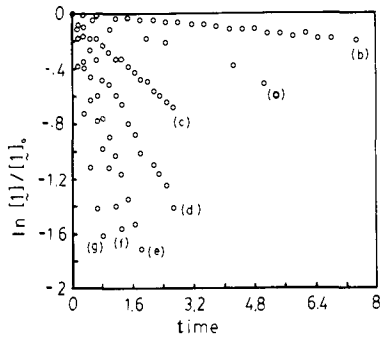

Figure 3. Kinetics of benzene elimination from $(C_5Me_5)Rh(PMe_2CH_2Ph)(C_6H_5)H$ in C_6D_6 (time in h except for part a, which is in days: (a) 295.7 K, (b) 310.7 K, (c) 320.7 K, (d) 324.4 K, (e) 329.2 K, (f) 332.0 K, (g) 334.7 K).

only slightly higher than $\Delta H°$ in eq 3 for intermolecular benzene activation by the unsaturated metal complex **3**, and the thermodynamic driving force for the favorability of **2** plus benzene over **1** is probably largely due to differences in $\Delta S°$. The large value of the equilibrium constant prevents the accurate extraction of $\Delta H°$ and $\Delta S°$ for eq 5 by measurement of the temperature dependence of K_{eq}.

B. Kinetics of Intra- and Intermolecular Aromatic C–H Bond Activation. The loss of benzene from **1** can be followed easily by heating the complex in C_6D_6 solution and monitoring the rate of disappearance of the ortho hydrogens of the rhodium-bound phenyl group. The equilibria and rate constants involved are shown in eq 5. A logarithmic plot of the area of the phenyl hydrogens of [**1**] vs. time gives a straight line with slope equal to $-k_1$ since once benzene is lost it is either replaced by C_6D_6 or the intermediate **3** undergoes cyclometalation to form **2**. The rate was monitored at several different temperatures as shown in Figure 3. *Qualitatively, C_6D_6 exchanges into the molecule about twice as fast as orthometalation occurs.* Also, since C_6D_6 is lost from $(C_5Me_5)Rh(PMe_2CH_2Ph)(C_6D_5)D$ faster than C_6H_6 is lost from **1** ($k_D = 2k_H$), this single experiment could not be used to also determine the overall rate of formation of **2** from **1**. The faster reductive elimination of C_6D_6 from $(C_5Me_5)Rh(PMe_2CH_2Ph)(C_6D_5)D$ results in a downward curvature of a plot of ln [**2**] vs. time.

Consequently, the rate of formation of **2** from **1** was determined by heating **1** in 95:5 C_6H_6:C_6D_6 (to permit NMR lock) and monitoring the disappearance of the integrated intensity of the C_5Me_5 resonance for **1** with time.[8] Application of the steady-state

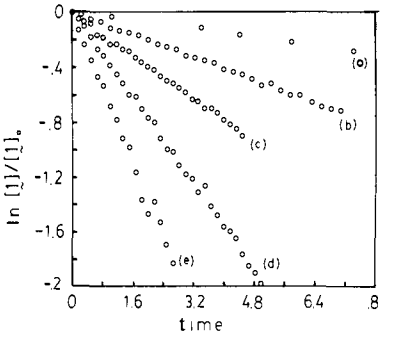

Figure 4. Kinetics of cyclometalation of $(C_5Me_5)Rh(PMe_2CH_2Ph)(C_6H_5)H$ in 95:5 C_6H_6:C_6D_6 (time in h except for part a, which is in days: (a) 295.7 K, (b) 320.0 K, (c) 324.4 K, (d) 329.2 K, (e) 333.8 K).

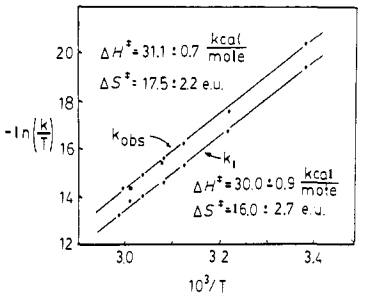

Figure 5. Eyring plot for the benzene elimination from and cyclometalation of $(C_5Me_5)Rh(PMe_2CH_2Ph)(C_6H_5)H$. The solid circles represent the rate constants that include the deuterium isotope effects due to exchange with C_6D_6.

approximation to the concentration of **3** in eq 5 gives the exact expression for the disappearance of **1** with time (eq 7). Now K_{eq}

$$\frac{-d[\mathbf{1}]}{dt} = k_1[\mathbf{1}] - k_{-1}[C_6H_6]\frac{k_1[\mathbf{1}] + k_{-2}[\mathbf{2}]}{k_{-1}[C_6H_6] + k_2} \qquad (7)$$

$= 36.7 = k_1k_2/(k_{-1}k_{-2}[C_6H_6])$, and since in neat benzene $k_{-1}[C_6H_6] \approx 2k_2$, $k_1 \approx 74k_{-2}$. Therefore the k_{-2} term can be neglected in the numerator of eq 7, giving the simplified form shown in eq 8. A plot of ln [**1**] vs. time was linear with slope $-k_{obsd}$ as defined in eq 8 and is shown in Figure 4 at several temperatures.

$$\frac{d[\mathbf{1}]}{dt} = -k_{obsd}[\mathbf{1}] = -k_1[\mathbf{1}]\frac{k_2}{k_2 + k_{-1}[C_6H_6]} \qquad (8)$$

The temperature dependence of the rate constants k_1 and k_{obsd} (Table II) can now be used to determine the temperature dependence of the difference between the free energies of activation in eq 3 and 4, $\Delta\Delta G^‡ = \Delta G^‡_4 - \Delta G^‡_3$. In turn, the temperature dependence of $\Delta\Delta G^‡$ allows the extraction of the difference between the individual activation parameters $\Delta\Delta H^‡$ ($=\Delta H^‡_4 - \Delta H^‡_3$) and $\Delta\Delta S^‡$ ($=\Delta S^‡_4 - \Delta S^‡_3$). As will be seen, both of these quantities are small compared to the errors in their measurement, and the analysis used in obtaining these values is outlined below.

The difference $\Delta\Delta G^‡$ is given by eq 9, and the ratio of the inter- and intramolecular rates is given by eq 10. Now the expression

$$\Delta\Delta G^‡ = RT \ln\{(\text{rate inter})/(\text{rate intra})\} \qquad (9)$$

$$(\text{rate inter})/(\text{rate intra}) = k_{-1}[C_6H_6][\mathbf{3}]/k_2[\mathbf{3}] \qquad (10)$$

(6) Since the conventional standard states for **1** and **2** are solids at 25 °C, it is assumed here that the free energies of solution and heat capacities of **1** and **2** are identical.

(7) (a) In comparing angle C1–C2–C7 to angle C3–C2–C7, a difference of 5.3° is observed which corresponds to a $\Delta\theta = 2.6°$ deviation from ideality. The strain energy in the C1–C2–C7 bond angle can be estimated at only ≈0.05 kcal/mol.[7b] Since this strain energy must be equal in all five of the cyclic bond angles, the total strain energy in the ring is approximately 0.3 kcal/mol. (b) Estimated by using a force constant of 0.17 kcal/mol/deg^2 from the MM2 program of N. L. Allinger (Program No. 318, Quantum Chemistry Program Exchange, Indiana University, Bloomington, IN), in the equation $E = 0.0438(k\Delta\theta^2)$.

(8) The small amount of C_6D_6 incorporation into **1** at long reaction times (5% max) did not produce a noticible curvature in the plots in Figure 4. As shown by the solid circles in Figure 5, substantial exchange with C_6D_6 does slightly displace the temperature-dependent behavior of k_{obsd}.

Table I ^{1}H NMR Spectral Data

compound	solvent	resonances, δ
$(C_5Me_5)Rh(PMe_2CH_2Ph)Br_2$	$CDCl_3$	1.833 (d, J = 2.2 Hz, 15 H) 1.482 (d, J = 10.8 Hz, 6 H) 3.535 (d, J = 9.2 Hz, 2 H) 7.115 (d, J = 7.2 Hz, 2 H) 7.260 (t, J = 6.4 Hz, 1 H) 7.328 (t, J = 7.3 Hz, 2 H)
$(C_5Me_5)Rh(PMe_2CH_2Ph)PhBr$	$CDCl_3$	1.645 (d, J = 2.6 Hz, 15 H) 1.135 (d, J = 9.8 Hz, 3 H) 1.245 (d, J = 9.7 Hz, 3 H) 3.073 (dd, J = 14.4, 8.8 Hz, 1 H) 3.253 (dd, J = 14.4, 8.8 Hz, 1 H) 6.917 (t, J = 7.1 Hz, 2 H) 7.195 (t, J = 7.1 Hz, 1 H) 7.253 (d, J = 6.5 Hz, 2 H) 6.985 (m, 3 H) 7.159 (br s, 1 H) 7.942 (br s, 1 H)
$(C_5Me_5)Rh(PMe_2CH_2Ph)PhH$ (**1**)	C_6D_6	1.801 (br s, 15 H) −13.405 (dd, J = 48.5, 32.5 Hz, 1 H) 1.839 (d, J = 9.3 Hz, 3 H) 1.875 (d, J = 9.2 Hz, 3 H) 2.761 (dd, J = 14.3, 8.1 Hz, 1 H) 2.836 (dd, J = 14.3, 9.1 Hz, 1 H) 7.01 (m, 3 H) 7.12 (m, 3 H) 7.672 (d, J = 7.0 Hz, 2 H)[a]
$(C_5Me_5)\overline{Rh(PMe_2CH_2C_6H_4)}H$ (**2**)	C_6D_{12}	1.900 (d, J = 2.2 Hz, 15 H) −13.397 (dd, J = 44.2, 31.6 Hz, 1 H) 1.334 (d, J = 9.9 Hz, 3 H) 1.393 (d, J = 10.8 Hz, 3 H) 2.763 (dd, J = 15.1, 9.6 Hz, 1 H) 2.874 (dd, J = 24.5, 9.2 Hz, 1 H) 6.605 (t, J = 7.2 Hz, 1 H) 6.698 (t, J = 7.4 Hz, 1 H) 6.795 (d, J = 7.3 Hz, 1 H) 7.259 (d, J = 7.7 Hz, 1 H)
$(C_5Me_5)\overline{Rh(PMe_2CH_2C_6H_4)}Br$	$CDCl_3$	1.712 (d, J = 2.8 Hz, 15 H) 1.496 (d, J = 9.2 Hz, 3 H) 1.729 (d, J = 10.8 Hz, 3 H) 3.072 (ddd, J = 14.4, 14.4, 1.3 Hz, 1 H) 3.172 (dd, J = 15.3, 8.8 Hz, 1 H) 6.850 (t, J = 7.3 Hz, 1 H) 6.962 (t, J = 7.4 Hz, 1 H) 7.050 (d, J = 7.3 Hz, 1 H) 7.485 (d, J = 7.7 Hz, 1 H)
$(C_5Me_5)Rh(PMe_2Pr)Br_2$	$CDCl_3$	1.785 (d, J = 3.3 Hz, 15 H) 1.041 (t, J = 7.3 Hz, 3 H) 1.592 (m, 2 H) 1.679 (d, J = 11.1 Hz, 6 H) 2.004 (m, 2 H)
$(C_5Me_5)Rh(PMe_2Pr)PhBr$	$CDCl_3$	1.606 (d, J = 2.5 Hz, 15 H) 0.954 (t, J = 7.2 Hz, 3 H) 1.295 (d, J = 10.2 Hz, 3 H) 1.364 (d, J = 10.0 Hz, 3 H) 1.427 (m, 2 H) 1.794 (m, 2 H) 6.924 (m, 3 H) 7.089 (br s, 1 H) 7.942 (br s, 1 H)
$(C_5Me_5)Rh(PMe_2Pr)PhH$ (**4**)	C_7D_{14}	1.787 −13.773 (dd, J = 48.4, 32.0 Hz, 1 H) 0.909 (t, J = 6.8 Hz, 3 H) 0.971 (d, J = 9.5 Hz, 3 H) 1.204 (d, J = 9.3 Hz, 3 H) 1.411 (m, 4 H) 6.691 (m, 3 H) 7.245 (d, J = 6.5 Hz, 2 H)
$(C_5Me_5)\overline{Rh(PMe_2CH_2CH_2C_6H_4)}Br$	C_6D_6	1.525 (d, J = 2.5 Hz, 15 H) 0.834 (d, J = 9.5 Hz, 3 H) 1.533 (d, J = 9.0 Hz, 3 H)[a]
$(C_5Me_5)\overline{Rh(PMe_2CH_2CH_2C_6H_4)}H$ (**5**)	C_7D_{14}	1.853 (br s, 15 H) −14.672 (dd, J = 43.1, 31.8 Hz, 1 H) 1.203 (m, 2 H) 1.276 (d, J = 10.2 Hz, 3 H) 1.356 (d, J = 9.2 Hz, 3 H) 1.618 (m, 2 H)[a]
$(C_5Me_5)Rh(PMe_2Pr)(Pr)H$ (**7**)	THF-d_8/C_6D_6 2:1	1.797 (d, J = 2.0 Hz, 15 H) −14.111 (dd, J = 50.0, 39.9 Hz, 1 H) 0.920 (t, J = 7.0 Hz, 3 H) 1.000 (d, J = 10 Hz, 3 H)[a]
$(C_5Me_5)Rh(PMe_2Pr)H_2$ (**8**)	C_7D_{14}	1.971 (br s, 15 H) −14.166 (dd, J = 41.0, 29.3 Hz, 2 H) 0.979 (t, J = 6.7 Hz, 3 H) 1.186 (d, J = 9.2 Hz, 6 H) 1.393 (m, 4 H)

[a] Remaining resonances not observed due to multiple diasteriotopic couplings or overlap with residual solvent.

for k_{obsd} defined in eq 8 can be rearranged as in eq 11, and substitution of eq 10 and 11 into eq 9 gives eq 12, which expresses $\Delta\Delta G^{\ddagger}$ as a function of the measured quantities k_1 and k_{obsd}.

$$\frac{k_1}{k_{obsd}} - 1 = \frac{k_{-1}[C_6H_6]}{k_2} \tag{11}$$

$$\Delta\Delta G^{\ddagger} = RT \ln\left(\frac{k_1}{k_{obsd}} - 1\right) \tag{12}$$

Both k_1 and k_{obsd} can be fit to the Eyring equation (eq 13) to give the activation parameters associated with their temperature-dependent rate constants. These two plots are shown in Figure 5. While activation parameters for k_1 reflect the reductive elimination and dissociation of coordinated benzene from **1**,[4a,c] the activation parameters for k_{obsd} involve both the **1** ⇌ **3** equilibrium and the **3** → **2** cyclometalation and do not have any simple physical interpretation. They are of use, however, in generating values of k_1 and k_{obsd} at different temperatures for use in determining $\Delta\Delta G^{\ddagger}$ from eq 12.

$$k = \frac{RT}{Lh} \exp\left(\frac{-\Delta H^{\ddagger}}{RT} + \frac{\Delta S^{\ddagger}}{R}\right) \tag{13}$$

Table II. Rate Data for k_1 (in C_6D_6) and k_{obsd} (in 95:5 C_6H_6:C_6D_6) (s^{-1})

	T,[a] K	k_{obsd}	k_1
1	295.7	4.06 (13) × 10^{-7}	1.093 (47) × 10^{-6}
2	310.7	7.27 (30) × 10^{-6} [b]	1.721 (83) × 10^{-5}
3	320.0	2.863 (27) × 10^{-5}	7.092 (77) × 10^{-5}
4	324.4	6.721 (67) × 10^{-5} [b]	1.363 (30) × 10^{-4}
5	324.4	9.52 (39) × 10^{-5} [c]	
6	324.5	5.42 (13) × 10^{-5}	1.470 (33) × 10^{-4}
7	329.2	1.098 (8) × 10^{-4}	2.527 (45) × 10^{-4}
8	332.0	3.10 (2) × 10^{-4} [d]	3.10 (2) × 10^{-4} [d]
9	332.0	1.864 (37) × 10^{-4} [b]	3.265 (63) × 10^{-4}
10	333.8	1.893 (30) × 10^{-4}	
11	334.7		5.81 (22) × 10^{-4}

[a] Uncertainty in T is ±0.15 °C. [b] k_{obsd} calculated from reaction in C_6D_6 with use of data from the first half of $\tau_{1/2}$ of the arene exchange reaction. (These data are shown by the solid circles in Figure 5.) [c] Reaction performed in C_6H_6/C_6D_{12} ($\chi_{benzene}$ = 0.264 (9)). [d] Reaction performed in C_6D_{12}.

Table III. Bond Distances (Å) and Angles (deg) for $(C_5Me_5)\overline{Rh(PMe_2CH_2C_6H_4)}Br$

Rh-Br	2.517 (1)	P-C7	1.815 (5)	C1-C2	1.395 (6)
Rh-P	2.249 (1)	P-C8	1.795 (5)	C2-C7	1.504 (7)
Rh-C1	2.046 (4)	P-C9	1.815 (5)		
Br-Rh-P	95.99 (4)	Rh-C1-C2	121.6 (3)	C7-P-Rh	102.3 (2)
Br-Rh-C1	89.6 (1)	C1-C2-C7	116.9 (4)	C3-C2-C7	122.2 (5)
P-Rh-C1	78.2 (1)	C2-C7-P	104.5 (3)		

Table IV. Calculated Values of $\Delta\Delta G^{\ddagger}$ vs. Temperature in Benzene

temp, °C	$\Delta\Delta G^{\ddagger}$, kcal/mol	(rate inter)/(rate intra)
25	0.368	1.86
30	0.346	1.78
40	0.302	1.62
50	0.255	1.49
60	0.207	1.37

Several calculated values of $\Delta\Delta G^{\ddagger}$ as a function of temperature over the range 25–60 °C are given in Table IV. The individually measured ratios of k_1/k_{obsd} at a single temperature could also be used to determine $\Delta\Delta G^{\ddagger}$ at that temperature, but some measurements of k_{obsd} and k_1 were made independently at different temperatures and would have to be excluded in this type of analysis.

The temperature dependence of the values of $\Delta\Delta G^{\ddagger}$ in Table IV allows the evaluation of $\Delta\Delta S^{\ddagger}$ since $d(\Delta G)/dT = -\Delta S$; furthermore, $\Delta\Delta H^{\ddagger}$ is obtained from the relation $\Delta\Delta H^{\ddagger} = \Delta\Delta G^{\ddagger} + T\Delta\Delta S^{\ddagger}$. These values for the difference in the activation parameters between eq 3 and 4 are $\Delta\Delta H^{\ddagger} = 1.7 \pm 0.8$ kcal/mol and $\Delta\Delta S^{\ddagger} = +4.5 \pm 2.5$ eu for the reaction in neat benzene solvent.[9] These experiments suggest, therefore, that there is a slight entropic favorability for an intramolecular C–H bond activation compared to an intermolecular activation of benzene solvent and that this entropic favorability is offset by an unfavorable enthalpic term. At 25 °C, $\Delta\Delta G^{\ddagger} = 0.37$ kcal/mol in benzene solvent and the coordinatively unsaturated intermediate **3** activates the intermolecular C–H bonds of the benzene solvent 1.86 times faster than it cyclometalates.

The above analysis applies to the state in which the intermolecular oxidative addition reaction involves neat benzene. However, it is obvious from eq 5 that if the benzene concentration is reduced the intramolecular reaction will become more favorable until eventually it becomes the major mode of reaction of the 16-electron intermediate **3**. In order to account for this change in the free energy of the reaction a correction term for the change in the standard state under which $\Delta\Delta G^{\ddagger}$ was determined must be included as was done in eq 6. This correction term also involves the mole fraction of benzene in solution (eq 14). As before, the standard state of 1 M benzene lies 1.5 kcal/mol below that for neat benzene, so that $\Delta\Delta G^{\ddagger} = -1.13$ kcal/mol and the intramolecular cyclization is now favored 6.6:1 over the intermolecular reaction with 1 M benzene.

$$\Delta\Delta G^{\ddagger} = \Delta\Delta G^{\ddagger}(\text{neat benzene}) + RT \ln (\chi_{benzene}) \quad (14)$$

As a proof of the accuracy of this equation, a solution of **1** in a mixture of C_6H_6/cyclohexene ($\chi_{benzene}$ = 0.264, 2.86 M) was heated to 51.2 °C and the rate constant k_{obsd} determined (9.53 ± 0.39 × 10^{-5} s^{-1}). Since k_1 is calculated to be 1.28 × 10^{-4} s^{-1} at this temperature, the ratio k_1/k_{obsd} can be used in eq 12 to determine an observed free energy difference for the intra- vs. intermolecular reaction of −0.69 (4) kcal/mol (intramolecular cyclization is favored). This observed value is in excellent agreement with the value of −0.61 (4) kcal/mol calculated with eq 14 and indicates that the use of mole fraction in place of activity is valid;[10] that is, the solvent is near ideal. The change in $\Delta\Delta G^{\ddagger}$ is a purely entropic effect. In changing the mole fraction of benzene from 1.0 to 0.264, the probability of the intermediate **3** encountering a benzene molecule in solution decreases from unity to approximately 1 out of 4. Since entropy is related to probability by the Boltzman expression $S = R \ln$ (probability), the correction term for mole fraction in eq 14 is in fact a statistical correction for the change in entropy of the benzene.

The above discussion is an attempt to use thermodynamic quantities to evaluate the preference for intra- or intermolecular reactions. The term $\Delta\Delta H^{\ddagger}$ can be associated with the energetic requirements for forming the transition state; but what exactly does the $\Delta\Delta S^{\ddagger}$ term represent? Initially, it was expected that this term would evaluate the translational contribution to the activation barrier for bringing two molecules together to form one as opposed to having one molecule reacting with itself to form another. But in fact, the $\Delta\Delta S^{\ddagger}$ measured also includes any differences between rotational modes and statistical differences between reaction 4 and its intermolecular counterpart. While the intermolecular reactant molecules can acheive the proper orientation for reaction of any of its 6 C–H bonds, the intramolecular reactant can only acheive geometries that result in activation of 2 of its C–H bonds (a statistical factor of $R \ln 3$ in entropy). Therefore it is difficult to assess the physical meaning that is associated with the small $\Delta\Delta S^{\ddagger}$ term determined by these studies.

The thermodynamic quantities determined above do permit the calculation of the relative reactivity of the 16-electron intermediate toward intra- and intermolecular reactions under conditions in which both the solvent concentration and reaction temperature are varied. This predictive ability, after all, is what one would like to have for systems involving intra- and intermolecular C–H activation.

The free energy profile is shown in Scheme II for this system at 51.2 °C in neat benzene and includes the arene precoordination step that was previously found to be important in the rate-determining step for arene activation by this system (see the following section).[4a,c] One obvious feature of this diagram is that while intramolecular activation of the ortho hydrogen of the benzyl group is favored thermodynamically over intermolecular benzene activation, there is a slight kinetic preference for activation of benzene solvent over the intramolecular cyclometalation. This inversion of the kinetic and thermodynamic selectivity is not what was anticipated on the basis of many of the earlier studies.

C. Mechanism of Intramolecular C–H Bond Activation. The above results involving the rate of C–H bond activation in an intramolecular reaction require some comment as to the nature of the rate-determining transition state for the activation of the benzylic ortho C–H bond. As was determined in earlier studies, the rate-determining transition state for intermolecular arene C–H bond activation involves η^2 coordination of the aromatic ring prior to oxidative addition.[4] The intramolecular coordination of the

(9) Errors in $\Delta\Delta H^{\ddagger}$ and $\Delta\Delta S^{\ddagger}$ are estimated as the average of the errors in the plots of k_1 and k_{obsd} vs. T. Using only the k_1/k_{obsd} ratios for those experiments carried out at identical temperatures gives $\Delta\Delta H^{\ddagger} = 0.74 \pm 4.0$ kcal/mol and $\Delta\Delta S^{\ddagger} = 3.0 \pm 4.1$ eu.

(10) That is, the activity coefficient γ in the expression $\alpha = \gamma\chi$(benzene) is approximately unity.

Scheme II. Free Energy Profile for the Arene Derivatives of $(C_5Me_5)Rh(PMe_2CH_2C_6H_5)(C_6H_5)H$ at 51.2 °C in C_6H_6

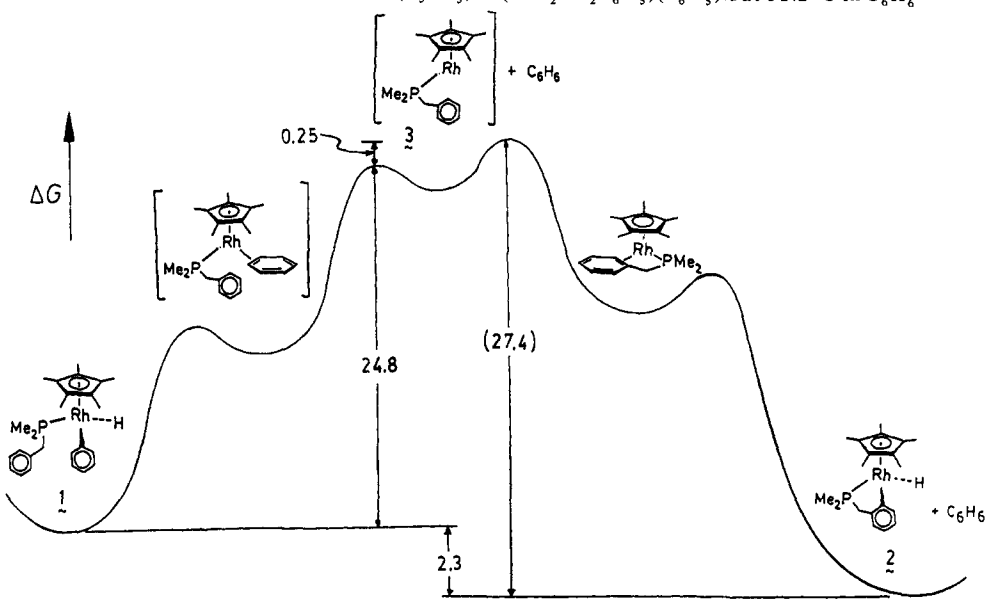

Scheme III. Proposed Mechanism for the Isomerization of $(C_5Me_5)Rh(PMe_2CH_2C_6H_4)D$

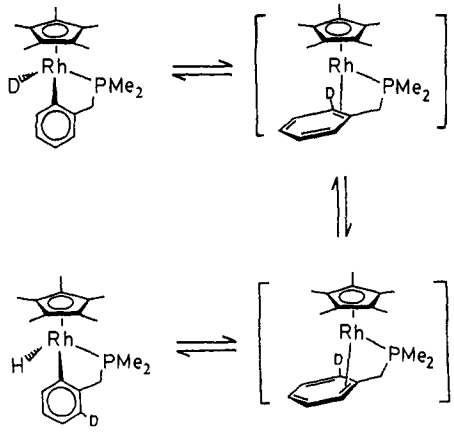

benzylic aromatic ring in **3** might have been anticipated to be unfavorable due to strain, thereby slowing the rate of intramolecular activation due to what can be attributed to an unfavorable steric effect; that is, $\Delta\Delta H^{\ddagger}$ might be expected to be greater than zero. The value of $\Delta\Delta H^{\ddagger}$ found in the previous section is only slightly positive, suggesting that there is no large difference in the strain energies for formation of the transition states of the intermolecular and intramolecular arene coordination.

The intermediacy of such an η^2 arene derivative can be demonstrated by treating the compound $(C_5Me_5)Rh(PMe_2CH_2C_6H_4)Br$ with Ag^+ in THF-d_8 solution followed by $Li^+[DBEt_3]^-$ at −40 °C. This procedure produces the complex $(C_5Me_5)Rh(PMe_2CH_2C_6H_4)D$, which upon warming above 15 °C equilibrates with the isomer $(C_5Me_5)Rh(PMe_2CH_2C_6H_3D)H$ (eq 15). Since temperatures of >50 °C

(15)

are required to dissociate the arene in complexes such as **1** or **2**, an isomerization must be occurring below room temperature. This process is shown in Scheme III and includes not only a step involving reversible reductive elimination to form an η^2-arene complex of the phosphine benzyl group but also a [1,2] shift of the coordinated double bond. This same type of isomerization process was also reported earlier in the complex $(C_5Me_5)Rh(PMe_3)(p\text{-}C_6H_3Me_2)D$ (in which the metal must migrate past an aromatic methyl group) and was found to have a slightly higher barrier than that for the aryl-hydride/η^2-arene complex interconversion[4a,c]. As the approximate temperature for this interconversion is the same in both **3**-d_1 and the previously reported *p*-xylyl complex, the steric effects associated with the formation of the intramolecular η^2-arene complex in the transition state must be small, so that $\Delta\Delta G^{\ddagger}$ is virtually unaffected by the small $\Delta\Delta H^{\ddagger}$ difference.

D. Comparison with Alkane Activation. The comparison of these selectivities for arene activation with those for alkane activation was examined by preparing the complex $(C_5Me_5)Rh(PMe_2CH_2CH_2CH_3)Br_2$ and converting it to the phenyl derivative by treatment with phenylmagnesium bromide. Further reaction of the $(C_5Me_5)Rh(PMe_2CH_2CH_2CH_3)(C_6H_5)Br$ with 1 equiv of $Na^+[H_2Al(OCH_2CH_2OMe)_2]^-$ yielded the complex $(C_5Me_5)Rh(PMe_2CH_2CH_2CH_3)(C_6H_5)H$ (**4**) in high yield (85%). Upon heating **4** at 58.8 °C in methylcyclohexane-d_{14} the equilibrium between **4** and the cyclometalated species $(C_5Me_5)Rh(PMe_2CH_2CH_2CH_2)H$ (**5**) plus benzene was established. The appropriate rate constants and intermediates for this equilibration are shown in eq 16. Accurate determination of the equilibrium

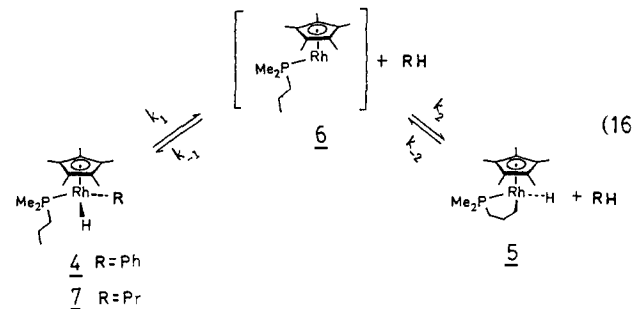

(16)

4 R=Ph
7 R=Pr

constant requires not only measurement of the ratio of **4**:**5** but also the concentration of the small amount of benzene present. The former ratio was found to be 0.43:1 and the latter concentration determined by quenching the solution with concentrated H_2SO_4 and determining the total $[C_6H_6]$ by gas chromatography (0.0307 (13) M). The calculated mole fraction equilibrium constant ($\chi_{benzene}$ = 0.00200) was found to be 4.59 (4) × 10^{-3} at 58.8 °C (molar K_{eq} = 0.0491 M). Upon heating the reaction to 80 °C, the ratio of **4**:**5** changed to 1:4 before undergoing slow

Table V. Bond Distances (Å) and Angles (deg) for $(C_5Me_5)Rh(PMe_2CH_2CH_2\dot{C}H_2)Br$

Rh–Br	2.517 (1)	P–C11	1.810 (11)	C13–C14	1.412 (15)
Rh–P	2.231 (3)	P–C12	1.813 (11)	C14–C15	1.456 (14)
Rh–C15	2.123 (9)	P–C13	1.786 (11)		
Br–Rh–P	91.33 (8)	Rh–C15–C14	116.3 (8)	C13–P–Rh	107.1 (6)
Br–Rh–C15	88.7 (3)	C15–C14–C13	117.1 (1)	C11–P–C13	104.4 (6)
P–Rh–C15	79.9 (3)	C14–C13–P	110.9 (9)	C12–P–C13	106.5 (5)

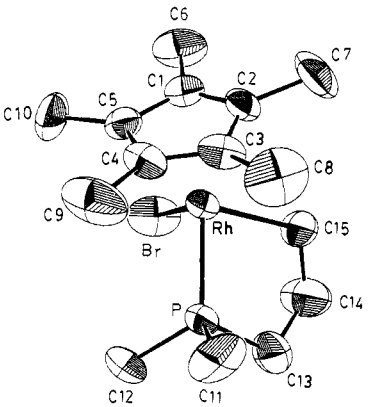

Figure 6. ORTEP drawing of $(C_5Me_5)\dot{R}h(PMe_2CH_2CH_2\dot{C}H_2)Br$. The ellipsoids are shown at the 50% proability level.

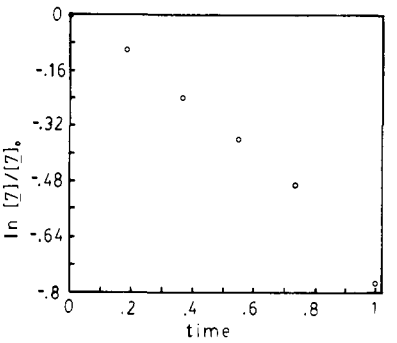

Figure 7. Kinetics of propane elimination from $(C_5Me_5)Rh(PMe_2Pr)(CH_2CH_2CH_3)H$ at 246.8 K in THF-d_8/C_6D_6.

Scheme IV. Free Energy Profile for the Alkane Derivatives of $(C_5Me_5)Rh(PMe_2Pr)(CH_2CH_2CH_3)H$ ((1) −55 °C, (2) −26.4 °C, (3) 25.3 °C)

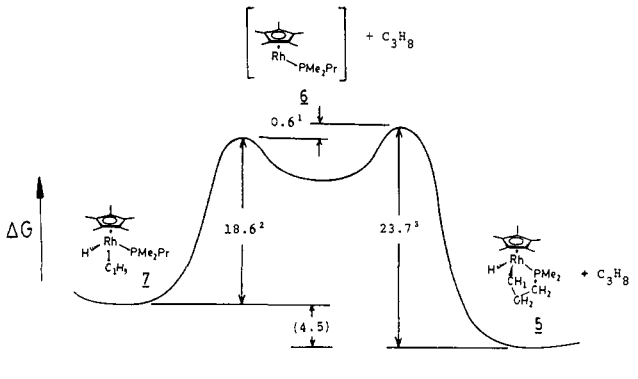

decomposition, qualitatively indicating that $\Delta S°$ for the equilibrium is positive. The cyclometalated complex is obviously much more stable than the other known rhodium alkyl-hydride complexes,[4b,c] although aromatic hydrocarbons are still highly favored thermodynamically by the 16-electron intermediate **6**.

Compound **5** is conveniently prepared by heating a solution of **4** in methylcyclohexane-d_{14} to 90 °C for 30 min and rapidly cooling to −196 °C. The ^1H NMR spectrum of **5** at high temperatures (>50 °C) shows broadening of the hydride resonance at δ −14.166, presumably due to the rapid reversibility of the reactions in eq 16. Compound **5** shows a remarkable overall stability compared to the alkyl hydride complexes studied earlier[4b,c] and nicely demonstrates the increased thermodynamic stability of intramolecularly activated alkyl groups. Quenching of the reaction solution with $CHBr_3$ permits isolation of the complex $(C_5Me_5)\dot{R}h(PMe_2CH_2CH_2\dot{C}H_2)Br$. An X-ray structural study of the molecule confirms the activation of the terminal C–H bond (Figure 6). Table V contains important bond distances and angles.

All attempts to equilibrate **5** with neat alkane solvent failed due to the instability of the alkyl-hydride complexes above −20 °C. Three separate experiments were performed that allowed a comparison of the relative stabilities of the intramolecularly activated species **5** and the intermolecularly activated complex $(C_5Me_2)Rh(PMe_2Pr)(CH_2CH_2CH_3)H$ (**7**).

The kinetic selectivity of **6** for propane vs. the phosphine propyl group was investigated by irradiation of $(C_5Me_5)Rh(PMe_2Pr)H_2$ (**8**) in liquid propane solvent at −55 ± 5 °C. After removal of the excess propane solvent at −78 °C, THF-d_8 and C_6D_6 (2:1) were added. A low-temperature ^1H NMR spectrum revealed the presence of two products, **5** and **7**, in 30% yield (1:4 ratio), as well as unreacted **8** (70%). Upon warming the solution to −26.4 °C, a slow first-order elimination of propane from **7** was observed (k = 1.87 (13) × 10^{-4} s^{-1}), which corresponds to an activation barrier of 18.6 kcal/mol (Figure 7) for propane reductive elimination from **7**.

For comparison, the cyclometalated complex **5** (prepared by heating **4** in methylcyclohexane-d_{14} at 90 °C) was diluted with toluene-d_8 and allowed to undergo reductive elimination at 25.3 °C. A slow reaction occurred to form $(C_5Me_5)Rh(PMe_2Pr)(C_6D_4CD_3)D$ with a first-order rate constant of 2.57 (8) × 10^{-5} s^{-1}. This rate corresponds to a free energy of activation of 23.7 kcal/mol and is much slower at 25.3 °C than the corresponding reductive elimination of propane from **7** at −26.4 °C. If the relative selectivity of the 16-electron intermediate **6** toward intermolecular reaction with propane solvent vs. intramolecular reaction with the phosphine propyl group at 25 °C is taken to be 4:1 ($\Delta\Delta G^{\ddagger} \approx 0.6$ kcal/mol), then an estimate of the relative stabilities of **5** and **7** can be determined.

With use of the above estimate of the kinetic selectivity of **6** for intra- vs. intermolecular reaction, the free energy diagram shown in Scheme IV can be constructed. It should be pointed out that this is a composite representation of the true reaction coordinate in that the reaction kinetics were measured under different reaction conditions. Nevertheless, it is evident that **5** is substantially more thermodynamically stable than **7** at room temperature (by at least 4 kcal/mol in neat alkane solvent). Indeed, if the entropy of activation for elimination of propane from **7** is 5–20 eu,[11] then the difference in free energies between **5** and **7** becomes even larger. Just as with arenes, intramolecular reaction is favored thermodynamically but not kinetically.

E. Comparison with Other Studies. In order to compare these results with those made in other intramolecular reactions, some discussion of the different types of thermodynamically possible systems is useful. For example, it is important to determine whether the products observed in a given experiment reflect the kinetic selectivity ($\Delta\Delta G^{\ddagger}$) or the thermodynamic stability ($\Delta\Delta G°$).

(11) Okrasinski, S. J.; Norton, J. R. *J. Am. Chem. Soc.* **1977**, *99*, 295–297. Mays, M. J.; Simpson, R. N. F.; Stefanini, F. P. *J. Chem. Soc., A* **1970**, 3000–3002. James, B. R. "Homogeneous Hydrogenation"; Wiley-Interscience: New York, 1973; pp 290–293. Michelin, R. A.; Faglia, S.; Uguagliati, P. *Inorg. Chem.* **1983**, *22*, 1831–1834. Milstein, D. J. *J. Am. Chem. Soc.* **1982**, *104*, 5227–5228. Chan, A. S. C.; Halpern, J. *J. Am. Chem. Soc.* **1980**, *102*, 838–840. Hart-Davis, A. J.; Graham, W. A. G. *J. Am. Chem. Soc.* **1971**, *93*, 4388–4393.

It is commonly presumed that the thermodynamic stability of the product of a reaction ($\Delta G°$) will be reflected in the activation energy for the reaction ($\Delta G^{\ddagger}$). This is clearly not the case in the present study and should not be generally assumed without justification.

For studies of reactions whose products are determined by kinetic selectivities, the useful concept of "effective molarities" (EM) has been brought forth for comparison of the rate of an intramolecular reaction with that of a similar intermolecular reaction.[12] The effective molarity of an intramolecular reaction is obtained by dividing the first-order rate constant for the reaction by the second-order rate constant for a similar bimolecular reaction. Effective molarity has the units of M and corresponds to the rate ratio for intra- vs. intermolecular reaction that would be observed if the bimolecular reaction involved 1 M substrate. This concept is especially useful for comparing unimolecular reaction rates with bimolecular reaction rates that do not involve neat substrate, such as in S_N2 reactions or enzyme catalysis. For the current studies, the effective molarities can be obtained by multiplying the observed selectivity for the intramolecular reaction relative to the intermolecular reaction by the concentration of neat benzene (eq 17). For the arene studies, an effective molarity of only 5.5 M is seen, substantially less than that found for intramolecular reaction involving an enzyme ($\sim 10^6$ M)[13] or even an S_N2 reaction forming a cyclic ether (10^3–10^5 for 5- and 6-membered rings).[14] The alkane studies similarly give an EM value of only 3.3 M.

$$\mathrm{EM} = \frac{k_{\mathrm{intra}}}{k_{\mathrm{inter}}} = \frac{[\mathrm{intra}]}{[\mathrm{inter}]}[\mathrm{RH}] \qquad (17)$$

What factors are important, then, in determining the EM or more precisely the $\Delta\Delta G^{\ddagger}$ of an intramolecular reaction relative to its intermolecular counterpart? The $\Delta\Delta G^{\ddagger}$ that determines reaction selectivity can be broken down into an enthalpic ($\Delta\Delta H^{\ddagger}$) and an entropic ($\Delta\Delta S^{\ddagger}$) contribution. The enthalpic term will relate to any bond or strain energy differences between the intra- and intermolecular reaction and can either accelerate or decelerate an intramolecular reaction.[15] Cyclization to make 3- and 4-membered rings have been known to be unfavorable in organic reactions for years, presumably due to the increase in ring strain in the unimolecular cyclization. For the systems in the present study, measurement of $\Delta\Delta H^{\ddagger}$ indicates that this term contributes only a small amount toward the disfavoring of the intramolecular reaction. Similarly, Whitesides has found that the strain energy of the 4-membered platinacyclobutanes is small and does not contribute to the disfavoring of the intramolecular reaction.[2f] On the contrary, Marks has used the large strain energy ($\sim$15 kcal/mol) in a thorium metallocyclobutane to drive an intramolecular to intermolecular rearrangement, an equilibrium effect on $\Delta\Delta H°$.[1h] Strain energies can therefore render intramolecular reactions unfavorable and should not be neglected when comparing EM values. Unfavorable enthalpy terms also appear in 7–12-membered rings due to multiple unfavorable gauche H–H interactions, commonly referred to as the "medium ring effect".[14]

The other factor that contributes to the kinetic selectivity $\Delta\Delta G^{\ddagger}$ is the entropy difference $\Delta\Delta S^{\ddagger}$ between the intra- and intermolecular reaction. Over a dozen terms have been coined to describe this difference, and a complete discussion of this problem applied to enzyme catalysis has been summarized by Jencks.[12,13] The major contribution to the difference $\Delta\Delta S^{\ddagger}$ is generally associated with the translational entropy difference between a unimolecular and a bimolecular reaction. For the formation of small (5 to 6 membered) unstrained rings, the proximity effect for the increase in the rate of an intramolecular vs. an intermolecular reaction has been calculated by Jencks and Koshland to be near unity for solvents such as neat benzene and propane (eq 18). Additional entropic effects such as the loss of the 3 molecular rotations and the freezing out of internal isomers in the correct conformation for reaction result in large contributions to decreasing the $\Delta S^{\ddagger}$ of an intramolecular reaction, resulting in EM values of up to 10^8.

$$(\text{rate intra})/(\text{rate inter}) = [\mathrm{RH}]/12 \approx 1 \qquad (18)$$

The small selectivities for intramolecular activation vs. intermolecular activation in the studies reported here can be accommodated by evaluating the three major contributions to $\Delta\Delta G^{\ddagger}$: (1) the enthalpy differences (bond energy, ring strain, diaxial interactions) are small, (2) the translational entropy difference between the intramolecular reaction and the intermolecular reaction with neat solvent is negligible, and (3) the intermediates **3** and **6** do not freeze out conformations of the phosphine aryl or alkyl groups that predispose their C–H bonds to oxidative addition.

In comparison with other systems, Jencks has stated that intramolecular reactions are experimentally observed to be about 10^5 faster than the analogous intermolecular reaction involving 1 M substrate.[13] This conclusion is based upon model systems involving ester hydrolysis studies and is said to apply to both kinetic and thermodynamic comparisons of "nonspecial" systems (i.e., non-enzyme-like). This magnitude of difference is clearly *not* the case with the activation of C–H bonds by the low-valent rhodium complexes studied here. What we suggest is that these rhodium studies serve as a better model for C–H bond activation by low valent transition metals than does ester hydrolysis in aqueous solution. The effect of ionic intermediates in the latter studies is certainly cause for concern (see ref 13, pp 287–296), especially when extrapolating to nonpolar transition-metal systems.

The lack of intermolecular alkane activation in the Pt system has been most recently prescribed to nonbonded steric interactions of the alkane with the [$LPtR_2$] species (a $\Delta\Delta H^{\ddagger}$ effect) and not due to any inherent entropic barrier.[5b] One can also ask whether the Werner intermediate (η^6-C_6H_6)Ru[P(*i*-Pr)$_3$] is capable of intermolecular activation of alkane C–H bonds at low temperatures, since it activates arene C–H bonds intermolecularly and alkane C–H bonds intramolecularly.[2h]

Conclusion

The study described here allows a quantitative assessment of the kinetic and thermodynamic effect of intramolecularity upon aromatic and aliphatic C–H bond activation. Surprisingly, the kinetic selectivity in both cases favors intermolecular reaction over intramolecular when neat solvent is the competing reactant. That is, an intramolecular reaction in which the starting material is not predisposed to internal reaction (nor the product disfavored due to strain) is not favored (or disfavored) compared to an intermolecular reaction with a neat substrate. Second, a moderately high thermodynamic preference for intramolecular C–H bond activation was found for both alkyl and aromatic C–H bonds. Therefore, on the basis of these studies, the intuitive notion that unimolecular reactions (to form small unstrained rings) are favored over bimolecular reactions (involving neat substrate) is true in thermodynamic terms but not in reaction kinetics. The implication for C–H bond activation is that many of the systems that have been shown to intramolecularly activate alkane C–H bonds may also activate alkane C–H bonds intermolecularly but that the products may have been overlooked due to lack of thermal stability.

Experimental Section

General. Most of the halide-containing rhodium(III) complexes described here are air stable and can be handled in air once the reaction mixtures have been properly quenched. All of the rhodium hydride complexes reported are extremely sensitive toward oxygen and halogenated solvents, and operations involving these compounds were performed

(12) Jencks, W. P. "Catalysis in Chemistry and Enzymology"; McGraw-Hill: New York, 1969; p 10. Page, M. I.; Jencks, W. P. *Proc. Natl. Acad. Sci. U.S.A.* **1971**, *68*, 1678–1683. Page, M. I. *Chem. Soc. Rev.* **1973**, *2*, 295–323.

(13) Jencks, W. P. *Adv. Enzymol.* **1975**, *43*, 268–296.

(14) Illuminati, G.; Mandolini, L.; Bernardo, M. *J. Am. Chem. Soc.* **1975**, *97*, 4960–4966. Illuminati, G.; Mandolini, L.; Masci, B. *J. Am. Chem. Soc.* **1981**, *103*, 4142–4145. Illuminati, G.; Mandolini, L.; Masci, B. *J. Am. Chem. Soc.* **1977**, *99*, 6308–6312. Illuminati, G.; Mandolini, L.; Masci, B. *J. Am. Chem. Soc.* **1974**, *96*, 1422–1427.

(15) Jencks has discussed intramolecular rate acceleration due to steric compression in ref 13. See also ref 12.

(16) Isobe, K.; Bailey, P. M.; Maitlis, P. M. *J. Chem. Soc., Dalton Trans.* **1981**, 2003–2008.

under a nitrogen atmosphere, either on a high-vacuum line with modified Schlenk techniques or in a Vacuum Atmosphere Corporation dri-lab which was free of halogenated solvents. Rhodium trichloride (42.9%) was obtained as a generous loan from Johnson Matthey, Inc. Pentamethylcyclopentadiene, $Li^+[DBEt_3]^-$, $Li^+[HB(sec\text{-}Bu)_3]^-$, and $Na^+[H_2Al(OCH_2CH_2OCH_3)_2]^-$ were obtained from Aldrich Chemical Co. Pentamethylcyclopentadiene was vacuum distilled from CaH_2 (25 °C, 10^{-3} mm) prior to use. Propane was obtained from J. T. Baker Chemical Co. and was purified by 3 freeze–pump–thaw cycles before use. Magnesium turnings (99.98+%) were obtained from Reade Manufacturing Corp. Tetrahydrofuran, C_6D_6, and THF-d_8 were distilled from dark purple solutions of sodium benzophenone ketyl under vacuum. Aliphatic and aromatic hydrocarbon solvents were vacuum distilled from dark purple solutions of potassium benzophenone ketyl containing tetraglyme. Bromoform was purified by fractional crystallization and was degassed (3 cycles) before use. All alkyllithium and Grignard reagents were standardized immediately prior to use with 1.06 M *tert*-butyl alcohol/1,10-phenanthroline indicator.

High-field ^1H NMR (400.13 MHz) and ^{13}C NMR (100.62 MHz) spectra were recorded on a Bruker WH-400 NMR spectrometer. The temperature for the NMR experiments was regulated by a Bruker BVT-1000 temperature control unit (±0.1 °C). Absolute calibration at ambient temperature (±0.05 °C) was determined by passing dry air through the probe while monitoring the equivalence of both the inlet and outlet stream temperatures with calibrated thermometers. Relative calibration was determined by plotting the separation of the two resonances of standard methanol or ethylene glycol samples vs. the Pt sensor voltage of the BVT-1000 unit. Analytical GC was performed on a Hewlett-Packard 5710A gas chromatograph with a 10 ft × $^1/_8$ in. 5% SE-30/Chromosorb WAW column (46–130 °C). X-ray structural investigations were carried out on an Enraf-Nonius CAD-4 diffractometer coupled to a TEXRAY PDP-11 computer.

The complexes $(C_5Me_5)Rh(PMe_2R)Br_2$ (R = benzyl, propyl) were prepared by treatment of the dimer $[(C_5Me_5)RhBr_2]_2$ with PMe_2CH_2Ph or PMe_2Pr as previously described.[4] Similarly, conversion of the dihalide complexes to the aryl or alkyl halide complexes was carried out by treatment with Grignard or lithium reagents in a manner previously described.[4] NMR data for these new derivatives are included in Table I.

Preparation of $(C_5Me_5)Rh(PMe_2CH_2Ph)(C_6H_5)H$ (1) and $(C_5Me_5)Rh(PMe_2Pr)(C_6H_5)H$ (4). Complex **1** is typically prepared by addition of 0.5 mL of 0.5 N (0.125 mmol) $Li^+[H_2Al(OCH_2CH_2OCH_3)_2]^-$ to a THF solution (5 mL) of $(C_5Me_5)Rh(PMe_2CH_2Ph)(C_6H_5)Br$ (0.12 mmol). The THF was removed under vacuum to leave an orange gum which gradually turned yellow over a period of 15–30 min. The residue was dissolved in 0.15 mL of THF, diluted to 1 mL with hexane, and then flash chromatographed on a small column (15 × 20 mm) of silica gel with 5:1 (v:v) hexane/THF as eluent. Removal of solvent (25 °C, 10^{-2} mm) gave a pale yellow solid that was recrystallized from hexane (−78 °C) to give pale yellow crystals. The reaction is virtually quantitative by NMR spectroscopy, but slight losses during chromatography result in isolated yields of 85–95%.

An identical procedure with $(C_5Me_5)Rh(PMe_2Pr)(C_6H_5)Br$ results in the formation of **4** in high yield after flash chromatography.

Preparation and Kinetics of Cyclometalation of $(C_5Me_5)\overline{Rh(PMe_2CH_2C_6H_4)}H$ (2). A solution of freshly prepared **1** (5 mg, 0.013 mmol) in 0.4 mL of the appropriate solvent (C_6D_{12}, C_6D_6, or 95:5 (v:v) C_6H_6:C_6D_6) was transferred to an NMR tube fitted with a vacuum adaptor. After 1 freeze-pump-thaw cycle the tube was sealed under 600 mm of nitrogen, lowered into the NMR probe, and allowed to thermally equilibrate at the appropriate reaction temperature for 15 min before initiating the kinetics experiment.

In C_6D_{12} solvent the progress of the reaction was quantified by monitoring the integrated intensity of the C_5Me_5 resonance of **1** (δ 1.810, d, J = 1.3 Hz) relative to the sum of the intensities of the C_5Me_5 resonances for **1** and **2** (δ 1.900, d, J = 2.2 Hz). The same observed rate constant was obtained by monitoring the integrated intensity of the ortho Rh–phenyl resonance (δ 7.303, d, J = 6.9 Hz, 2 H) of **1** relative to Dow Corning silicone lubricant as an internal standard.

In C_6D_6 solvent the rate of formation of **2** (k_{obsd}) was quantified by monitoring the integrated intensity of the C_5Me_5 resonance for **1** relative to the sum of the intensities of the C_5Me_5 resonances for both **1** and **2**. The observed rate increased as the reaction progressed due to a facile C_6H_6/C_6D_6 exchange which produces the slightly more labile C_6D_6 complex.[4] The rate of C_6H_6 reductive elimination/dissociation (k_1) was obtained by monitoring the ortho Rh–phenyl resonances of **1** relative to the total integrated intensity of the C_5Me_5 resonances for **1** and **2**.

In 95:5 (v:v) C_6H_6/C_6D_6 the rate of formation of **2** and disappearance of **1** (k_{obsd}) was obtained by monitoring the integrated intensity of the C_5Me_5 resonance for **1** relative to the sum of the integrated intensities of the C_5Me_5 resonances for **1** and **2**. The large excess of C_6H_6 circumvented the problems associated with C_6D_6 arene exchange while permitting deuterium lock on the C_6D_6 resonance but necessitated the use of a homo-gated decoupling sequence to suppress the large C_6H_6 resonance. After long reaction time at 51.2 °C, the equilibrium position of the reaction mixture was composed of 97.7% **2** and 2.3% **1**.

A similar kinetics experiment was performed by monitoring the disappearance of **1** in 3.1:1 (v:v) C_6D_{12}/C_6H_6 ($\chi_{benzene}$ = 0.264 (9)) solvent. The composition of the solvent mixture was measured by gas chromatography.

Preparation of $(C_5Me_5)Rh(PMe_2Pr)H_2$ (8). This compound was prepared in a fashion analogous to that for the known $(C_5Me_5)Rh(PMe_3)H_2$.[16] $Na^+[H_2Al(OCH_2CH_2OCH_3)_2]^-$ (2.6 mL, 0.5 N, 5 equiv) was added to a suspension of $(C_5Me_5)Rh(PMe_2Pr)Br_2$ (0.26 mmol) in 5 mL of benzene. The mixture was stirred for 15 min at 25 °C and the volatiles removed to give a milky residue. The gum was dissolved in THF (0.5 mL) and hexane (2.5 mL) added to precipitate the salts. The mixture was flash chromatographed on SiO_2 (5:1 (v:v) hexane/THF) and the volatiles removed under vacuum (25 °C, 10^{-2} mm) to afford pale yellow **8** in 73% isolated yield.

Preparation and Reductive Elimination of $(C_5Me_5)Rh(PMe_2Pr)(CH_2CH_2CH_3)H$ (7). A solution of **8** (3 mg, 0.009 mmol) in liquid propane was irradiated at −40 °C in an NMR tube attached to a ground glass joint. The propane solvent was removed at −78 °C and THF-d_8 (0.3 mL) and C_6D_6 (0.15 mL) distilled into the tube. After the tube was sealed under vacuum, the sample was lowered into the probe of the NMR spectrometer which has been previously cooled to −50 °C. An NMR spectrum at −50 °C revealed the presence of three metal-containing compounds: **8** (70%; δ 1.933 (s, 15 H), 1.110 (d, J = 10 Hz, 6 H), 0.840 (t, J = 7.0 Hz, 3 H), −14.000 (dd, J = 50.0, 39.9 Hz, 2 H)), **5** (6%; δ 1.834 (d, J = 2.0 Hz, 15 H)), and **7** (24%; δ 1.797 (d, J = 2.0 Hz, 15 H), 1.000 (d, J = 10 Hz, 6 H), 0.920 (t, J = 7.0 Hz, 3 H), −14.111 (dd, J = 50.0, 39.9 Hz, 1 H)). The temperature of the sample was raised to −26.4 °C whereupon a rapid first-order reductive elimination of propane (δ 0.790, t, J = 7.0 Hz; δ 1.200, septet, J = 7.0 Hz) occurred. The rate constant $k = 1.87 \pm 0.13 \times 10^{-4}$ s^{-1} was obtained by monitoring the disappearance of the triplet resonance of **7** (δ 0.920) relative to Dow Corning silicon at δ 0.079.

Equilibration of $(C_5Me_5)Rh(PMe_2Pr)(C_6H_5)H$ (4) with Benzene. A solution of **4** (6 mg, 0.014 mmol) in methylcyclohexane-d_{14} (0.4 mL) was prepared as described above and transferred to an NMR tube fitted with a vacuum adapter. The tube was sealed under 600 mm of nitrogen and lowered into the NMR probe at 58.8 °C. The progress of the cyclometalation reaction was quantified by monitoring the integrated intensity of the C_5Me_5 resonances for **4** (δ 1.787) relative to the sum of the intensities of the C_5Me_5 resonances for **4** and **5** (δ 1.856). A least-squares fit of the relative intensity (C/C_0) of **5** to eq 19 with C_e = 0.0205 (3) M gives a rate constant for the loss of benzene from **4** of $1.64 \pm 0.04 \times 10^{-3}$ s^{-1} which is close to the experimental limits of the rate constant measured for the reductive elimination of benzene from **4** in C_6D_6 ($2.0 \pm 0.03 \times 10^{-4}$ s^{-1}). At 58.8 °C the experimentally measured ratio of **4**:**5** was 0.43:1. Upon warming the sample to 66 °C, the ratio decreased to 0.28:1. Slow sample decomposition at higher temperatures made it impossible to accurately determine the equilibrium constant as a function of temperature.

$$[C_0C_e + C(C_0 - C_e)]/[C_0(C_e - C)] = \exp[k(t + t_0)(2C_0 - C_e)/C_e] \quad (19)$$

where C_0 = initial concentration of **4**, C_e = equilibrium concentration of **5**, and C = concentration of **5** at time t

The concentration of benzene in each reaction mixture was determined by quenching the reaction mixture with concentrated H_2SO_4 and analyzing for total benzene by gas chromatography using naphthalene as internal standard. The total benzene concentration was found to be 0.0307 (13) M in the 58.8 °C reaction.

Reaction of $(C_5Me_5)\overline{Rh(PMe_2CH_2CH_2CH_2)}H$ (5) with Toluene-d_8. Compound **5** was prepared by heating a solution of **4** (7 mg, 0.017 mmol) in methylcyclohexane-d_{14} (0.4 mL) to 90 °C for 30 min in an NMR tube attached to a vacuum adapter. The tube was rapidly cooled to −196 °C and evacuated (10^{-4} mm), toluene-d_8 (0.2 mL) was added by vacuum distillation (25 °C, 10^{-4} mm), and the tube was sealed under vacuum. After the tube was warmed to −78 °C, the solvent was mixed thoroughly, and the sample was lowered into the NMR probe which had been previously cooled to −40 °C. A ^1H NMR spectrum of the reaction mixture revealed the presence of three major C_5Me_5-containing products: **5** (65%), **4** (30%), and **8** (5%). The temperature of the NMR probe was gradually raised until at 25.3 °C a slow first-order ($k = 2.57 \pm 0.08 \times$

Table VI. Summary of Crystallographic Data

crystal parameters	$(C_5Me_5)\overline{Rh(PMe_2CH_2C_6H_4)}Br$	$(C_5Me_5)\overline{Rh(PMe_2CH_2CH_2CH_2)}Br$
formula	$RhBrPC_{19}H_{27}$	$RhBrPC_{15}H_{27}$
fw	469.22	421.19
cryst system	triclinic	monoclinic
space group	$P\bar{1}$	$P2_1/n$
Z	2	4
a, Å	8.7937 (22)	13.0815 (130)
b, Å	15.0766 (33)	8.6933 (66)
c, Å	8.2527 (29)	15.2536 (99)
α, deg	105.08 (2)	90
β, deg	112.73 (2)	95.97
γ, deg	91.12 (2)	90
V, Å^3	964.1	1725.3
d_{calcd}, g/cm^3	1.616	1.621
xtal dimentions, nm	0.08 × 0.15 × 0.30	0.30 × 0.35 × 0.40
temp, °C	25	25
Measurement of Intensity Data		
diffractometer	Enraf-Nonius CAD4, κ geometry	
radiation	Mo, 0.71073 Å	
monochromator	graphite	
scan type	$2\theta/\omega$	
scan range	0.7 + 0.35 tan (θ)	
scan rate, deg/min	2.8–20	
total background time	scan time/2	
takeoff angle, deg	2.6	
2θ range, deg	2–40	2–40
data collected	$+h,\pm k,\pm l$	$+h,+k,\pm l$
no. of data collected	1805	2560
no. of unique data $>3\sigma$	1558	1164
no. of parameters varied	199	163
absorption coefficient, cm^{-1}	30.02	33.45
systematic absences	none	$h0l, h + l$ odd $0k0, k$ odd
equivalent data	$0kl = 0\bar{k}\bar{l}$	$0kl = 0k\bar{l}$
agreement between equiv data (based on F_{obsd}^2)	0.011	0.041
R	0.026	0.049
R_w	0.035	0.057
goodness of fit	1.43	2.09

10^{-5} s^{-1}) decrease in the integrated intensity of the C_5Me_5 resonance of **5** was observed.

Equilibration of $(C_5Me_5)\overline{Rh(PMe_2CH_2C_6H_4)}D$. A solution of $(C_5Me_5)\overline{Rh(PMe_2CH_2C_6H_4)}Br$ (9 mg, 0.019 mmol) and $Li^+[DBEt_3]^-$ (100 μL of a 1 M THF solution, 0.05 mmol) in 2 mL of THF was evaporated to give an orange gum which gradually turned pale yellow over a period of 5 min. The crude product was purified by flash chromatography (SiO_2, 5:1 hexane/THF). A ^1H NMR spectrum revealed that extensive H/D exchange had occurred between the proton at the 3-position of the aromatic ring (δ 7.80) and the deuterium at the metal center. The ratio of the integrated intensity of the metal hydride resonances to the 3-phenyl resonance was 26:25 and remained unchanged after 20 min at 25 °C.

Preparation of $(C_5Me_5)\overline{Rh(PMe_2CH_2C_6H_4)}Br$. A solution of **1** (73 mg, 0.156 mmol) in hexane (5 mL) was refluxed for 2 h. After the solution was cooled to 25 °C, $CHBr_3$ (100 μL, 1.1 mmol) was added and the solvent then removed (25 °C, 10^{-3} mm) to yield a bright orange residue. Recrystallization of the residue from hexane afforded reddish orange crystals of the product in 84% yield. Mass spectrum (20 eV): 468, 470 (M^+).

Preparation of $(C_5Me_5)\overline{Rh(PMe_2CH_2CH_2CH_2)}Br$. A solution of 4 (20 mg, 0.048 mmol) in hexane (7 mL) was heated for 15 min at 90 °C in a test tube which was fitted with a rubber septum. After the solution was cooled to 0 °C, $CHBr_3$ (50 μL, 0.57 mmol) was added. The hexane solvent was removed (25 °C, 10^{-3} mm) to give an orange residue which was purified by preparative thin-layer chromatography (SiO_2; 1% THF/CH_2Cl_2) and recrystallization from CH_2Cl_2/hexane. Yield: 56% (11 mg). ^{13}C NMR ($CDCl_3$): δ 9.452 (q, J = 128 Hz), 16.692 (qd, J = 127, 26 Hz), 16.778 (qd, J = 130, 27 Hz), 29.205 (td, J = 130, 10.7 Hz), 29.515 (tdd, J = 130, 23, 4.5 Hz), 97.443 (dd, J = 7.7, 4.6 Hz). Mass spectrum (20 eV): m/e 420, 422 (M^+).

X-ray Structural Determination of $(C_5Me_5)\overline{Rh(PMe_2CH_2C_6H_4)}Br$. Well-formed crystals of the cyclometalated phosphine derivative were prepared by slow evaporation of a hexane solution. The lattice constants were obtained from 25 centered reflections with values of χ between 10 and 45°. Cell reduction with the program TRACER revealed only a triclinic crystal system. Data were collected on the crystal in accord with the parameters in Table VI. The space group was assigned as $P\bar{1}$, and the correctness of this choice was confirmed by successful solution of the

Table VII. Positional Parameters and Their Estimated Standard Deviations for $(C_5Me_5)\overline{Rh(PMe_2CH_2C_6H_4)}Br$[a]

atom	x	y	z	B, Å^2
Rh	0.41939 (4)	0.26408 (2)	0.43599 (4)	2.464 (9)
Br	0.42432 (8)	0.34909 (4)	0.21237 (7)	4.73 (2)
P	0.6476 (2)	0.34867 (9)	0.6736 (2)	3.12 (3)
C1	0.6044 (5)	0.1933 (3)	0.3959 (6)	2.8 (1)
C2	0.7555 (6)	0.1964 (3)	0.5414 (6)	3.3 (1)
C3	0.8753 (6)	0.1422 (4)	0.5144 (7)	4.0 (1)
C4	0.8473 (6)	0.0861 (4)	0.3448 (8)	4.8 (2)
C5	0.7002 (7)	0.0827 (4)	0.1986 (7)	4.9 (2)
C6	0.5803 (6)	0.1365 (4)	0.2244 (6)	3.7 (1)
C7	0.7825 (6)	0.2612 (4)	0.7260 (7)	3.9 (1)
C8	0.7660 (7)	0.4289 (4)	0.6255 (8)	4.5 (2)
C9	0.6448 (7)	0.4138 (4)	0.8911 (7)	4.4 (2)
C10	0.1424 (6)	0.2675 (3)	0.3626 (6)	3.1 (1)
C11	0.2231 (6)	0.2765 (3)	0.5505 (6)	3.3 (1)
C12	0.3065 (6)	0.1947 (3)	0.5677 (6)	3.0 (1)
C13	0.2619 (5)	0.1347 (3)	0.3861 (6)	2.9 (1)
C14	0.1685 (6)	0.1808 (3)	0.2616 (6)	3.1 (1)
C15	0.0341 (7)	0.3327 (4)	0.2779 (7)	4.5 (2)
C16	0.2124 (6)	0.3517 (4)	0.7020 (7)	4.4 (1)
C17	0.3859 (7)	0.1676 (4)	0.7385 (7)	4.2 (1)
C18	0.3019 (6)	0.0391 (3)	0.3412 (7)	3.9 (1)
C19	0.0927 (7)	0.1442 (4)	0.0572 (7)	5.0 (2)

[a] Anisotropically refined atoms are given in the form of the isotropic equivalent thermal parameter defined as $(4/3)[a^2B(1,1) + b^2B(2,2) + c^2B(3,3) + ab(\cos\gamma)B(1,2) + ac(\cos\beta)B(1,3) + bc(\cos\alpha)B(2,3)]$.

Table VIII. Positional Parameters and Their Estimated Standard Deviations for $(C_5Me_5)Rh(PMe_2CH_2CH_2CH_2)Br$

atom	x	y	z	B, Å²
Rh	0.27554 (8)	0.2034 (1)	-0.00009 (6)	3.02 (2)
Br	0.2539 (1)	-0.0436 (2)	0.0820 (1)	6.53 (4)
P	0.2442 (3)	0.3424 (4)	0.1172 (2)	3.97 (8)
C15	0.427 (1)	0.221 (2)	0.0649 (9)	5.6 (4)
C13	0.358 (1)	0.337 (2)	0.193 (1)	7.2 (5)
C14	0.435 (1)	0.246 (2)	0.160 (1)	9.3 (6)
C11	0.217 (1)	0.545 (2)	0.102 (1)	7.3 (5)
C12	0.140 (1)	0.280 (2)	0.1779 (9)	6.7 (4)
C1	0.270 (1)	0.092 (2)	-0.1311 (8)	4.2 (3)
C2	0.3302 (9)	0.222 (2)	-0.1320 (7)	4.0 (3)
C3	0.268 (1)	0.351 (1)	-0.1146 (8)	4.2 (3)
C4	0.164 (1)	0.301 (2)	-0.1097 (7)	4.4 (3)
C5	0.1669 (9)	0.139 (1)	-0.1190 (8)	3.6 (3)
C6	0.302 (1)	-0.071 (2)	-0.146 (1)	7.0 (4)
C7	0.441 (1)	0.221 (2)	-0.1522 (9)	7.5 (5)
C8	0.301 (1)	0.514 (2)	-0.118 (1)	8.1 (5)
C9	0.071 (1)	0.397 (2)	-0.104 (1)	8.5 (5)
C10	0.079 (1)	0.036 (2)	-0.1187 (9)	7.3 (5)

Patterson map. The Molecular Structure Corporation SDP package was used for solution and refinement of the structure. A series of least-squares and difference Fourier maps revealed all 22 non-hydrogen atoms. Hydrogen atoms were placed with use of a difference Fourier map for methyl hydrogens or in idealized geometries for phenyl hydrogens. Final anisotropic refinement of all non-hydrogen atoms was carried out with fixed positional and thermal (B = 6.0) parameters for the 27 hydrogen atoms. Table III contains relevant bond distances and angles and Table VII positional parameters.

X-ray Structural Determination of $(C_5Me_5)Rh(PMe_2CH_2CH_2CH_2)Br$. Well-formed crystals of the cyclometallated phosphine derivative were prepared by slow evaporation of a hexane solution. The lattice constants were obtained from 25 centered reflections with values of χ between 10 and 45°. Cell reduction with the program TRACER revealed a monoclinic crystal system. The space group was assigned as $P2_1/n$ on the basis of systematic absences. Data were collected on the crystal in accord with the parameters in Table VI. The correctness of the choice of space group was confirmed by successful solution of the Patterson map. The Molecular Structure Corporation SDP package was used for solution and refinement of the structure. A series of least-squares and difference Fourier maps revealed all 18 non-hydrogen atoms. Hydrogen atoms were placed with use of a difference Fourier map for methyl hydrogens or in idealized geometries for phenyl hydrogens. Final anisotropic refinement of all non-hydrogen atoms was carried out with fixed positional and thermal (B = 6.0) parameters for the 27 hydrogen atoms. Table V contains relevant bond distances and angles and Table VIII lists positional parameters.

Acknowledgment. We thank Prof. Robert G. Bergman for helpful discussions with regard to the effect of standard states upon free energies, F.J.F. thanks the Messersmith Fund for financial support. This work was carried out under U.S. Department of Energy Grant No. 83ER13095. We also thank the Research Corporation and Chevron Research Corporation for their continued support of these studies.

Supplementary Material Available: Tables of thermal parameters, positional parameters of placed atoms, bond distances and angles, structure factors, and least-squares planes (41 pages). Ordering information is given on any current masthead page.

Reactions of $Re_2(CO)_8[\mu$-(L-L)] (L-L = dppm, dmpm) and $Re_2(CO)_7[\mu$-(L-L)](NCMe) with Alkynes[1]

Kang-Wook Lee,[2a] William T. Pennington,[2b] A. Wallace Cordes,[2b] and Theodore L. Brown*[2a]

Contribution from the School of Chemical Sciences, University of Illinois, Urbana-Champaign, Urbana, Illinois 61801, and the Department of Chemistry, University of Arkansas, Fayetteville, Arkansas 72701. *Received May 14, 1984*

Abstract: The photochemical reaction of $Re_2(CO)_8[\mu$-(L-L)] (L-L = dppm, dmpm) with terminal alkynes, RC≡CH (R = H, Ph), results in formation of $(\mu$-H)$Re_2(CO)_7[\mu$-(L-L)]$(\eta^1$-C≡C$Re_2)$ (I), $(\mu$-H)$Re_2(CO)_6[\mu$-(L-L)]$(\mu$-η^1,η^2-C≡CR) (II), $Re_2(CO)_5$(L-L)$(\mu$-η^1,η^2-C(R)=$CH_2)(\mu$-η^1,η^2-C≡CR) (III), and $Re_2(CO)_6[\mu$-(L-L)]$(\mu$-η^1,η^2-C(R)=$CH_2)(\mu$-η^1,η^2-C≡CR) (IV). The yield for each product depends on the reaction time and the bridging ligand. I is the first isolated example of bridging hydrido, σ-bonded alkynyl di- or polynuclear compounds directly formed from alkyne. In the reaction of II with acetylenes, coordination of dppm has been rearranged to form a chelate in III. The kinetic studies for the photochemical reactions of $Re_2(CO)_8[\mu$-(L-L)] and the isolated compounds I and II (L-L = dppm; R = Ph) with phenylacetylene indicate that the consecutive reactions occur with loss of one carbonyl ligand in each step: $Re_2(CO)_8(\mu$-dppm) → I → II → III. The reaction of $Re_2(CO)_8[\mu$-(L-L)] with Me_3NO in acetonitrile yields the acetonitrile-substituted complex $Re_2(CO)_7[\mu$-(L-L)](NCMe) (VI) wherein the acetonitrile ligand is located trans to phosphorus. The thermal reaction of VI with phenylacetylene at low temperature (40 °C) yields I, in which the σ-bonded alkynyl ligand is cis to phosphorus. In the case of the reaction of $Re_2(CO)_7(\mu$-dppm)(NCMe) with phenylacetylene, the isomer of I wherein σ-bonded alkynyl ligand is located trans to phosphorus is isolated as a minor product. I is transformed to II in a high-temperature thermal reaction (110 °C). The bridging alkynyl ligand of II undergoes a rapid fluxional process. The ΔG^*_c value estimated from the coalescence temperature in the ^{13}C NMR spectra is 10.5 kcal/mol. The structures of $(\mu$-H)$Re_2(CO)_7(\mu$-dmpm)$(\eta^1$-C≡CPh) (I_d) and $Re_2(CO)_5$(dppm)$(\mu$-η^1,η^2-CH=$CH_2)(\mu$-η^1,η^2-C≡CPh) (III_c) were determined by conventional crystallographic techniques with Mo Kα X-rays. The crystals of I_d belong to the monoclinic space group $P2_1/c$ with a = 12.594 (1) Å, b = 11.075 (1) Å, c = 18.461 (3) Å, β = 105.88 (1)°, V = 2476.8 (9) Å³, and z = 4. The crystals of III_c belong to the orthorhombic space group $Pbca$ with a = 12.743 (2) Å, b = 15.974 (2) Å, c = 35.174 (4) Å, V = 7160 (2) Å³, and Z = 8.

As part of a broadly based study of the photochemical properties of dirhenium carbonyl compounds, we have shown that the presence of a bridging phosphorus ligand such as bis(diphenylphosphino)methane (dppm), bis(dimethylphosphino)methane

0002-7863/85/1507-0631$01.50/0